

Human-Machine Interactive Control for Geared Mechatronic Systems by Using Load-side Encoder

Shota Yamada* Student Member, Hiroshi Fujimoto* Senior Member

Demands for robots working with human are increasing in industrial and welfare robotic fields. Cooperative robots have a lot of possibilities for proceeding factory automation and reducing welfare work burdens. They are required to be human-friendly; They need to be safe and follow human's intention flexibly. Recently, in industry, there is a trend toward the expansion of the use of load-side encoders thanks to their cost reduction. Based on this industrial trend, in this paper, a human-machine interactive control method for geared systems is proposed using the load-side encoder information and backlash. The advantages which can be obtained by applying an encoder to the load side of the cooperative robots are shown theoretically and quantitatively by simulations and experiments.

Keywords: Human-machine interaction, Backdrivability, Backlash, Load-side encoder, Cooperative robot, Two-inertia system

1. Introduction

Demands for robots working with human are increasing in industrial and welfare robotic fields⁽¹⁾. Cooperative robots have a lot of possibilities for proceeding factory automation and reducing welfare work burdens. They are required to be human-friendly; They need to be safe and follow human's intention flexibly.

Backdrivability is an important characteristic in cooperative robots. It indicates how easily mechatronic systems can be moved from their load sides. The main factors deteriorating backdrivability are motor-side impedance and friction amplified by a gear reducer. By enhancing backdrivability in industrial robots and welfare robots, workers can move the robots easily and arbitrarily in safety, which helps to improve working productivity and makes human-machine interaction possible.

Robots usually have gear reducers to miniaturize their whole systems⁽²⁾. For controlling the robotic systems, low resonance frequencies caused by low stiff gear reducers restrict their control bandwidths. Conventionally, the systems are modeled as two-inertia systems to consider their resonant characteristics, and a lot of studies are conducted aiming at higher control bandwidths⁽³⁾. Moreover, gear reducers have not only low stiffness but also nonlinearities such as backlashes, which deteriorate the precision of positioning at the load sides⁽⁴⁾. Backlash, the gap between teeth in a gear reducer, is known to be difficult to deal with. A lot of studies have been conducted regarding the compensation of backlashes⁽⁵⁾⁽⁶⁾.

To obtain high precise positioning at the load sides, the number of the devices with high resolution encoders at the load sides is increasing in industry. Also in robots' fields, it is easily expected that their reduction in cost will increase



Fig. 1. Outlook of the two-inertia system motor bench.

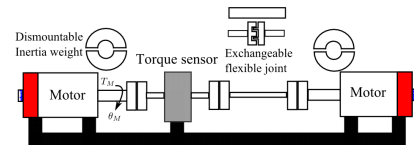


Fig. 2. Structure of the two-inertia system motor bench.

the use of load-side encoders. Therefore, we have developed a new robot module with a novel structure to equip with a load-side encoder in the literature⁽⁷⁾. Now, the developments of novel control methods using load-side encoder information are highly required

Our research group has proposed a high backdrivable control method using load-side encoder information and backlash actively⁽⁸⁾. Although backlash is known to be difficult to deal with, only from the view point of backdrivability, backlash has an ideal characteristic because the load side idles within the backlash width (i.e. When someone puts external force at the load side, the load side does not hit the motor side within the backlash width). This means that someone who puts external force from the load side only feels the load-side impedance without motor-side impedance. The proposed method uses this idling characteristic by implementing the precise position control of the motor side.

In this paper, to make human-machine interactive control

* The University of Tokyo
5-1-5, Kashiwanoha, Kashiwa, Chiba, 227-8561 Japan
Phone: +81-4-7136-3873
Email: yamada@hflab.k.u-tokyo.ac.jp

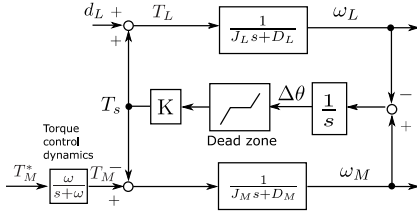


Fig. 3. Block diagram of the two-inertia system motor bench.

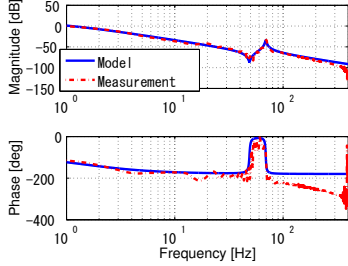


Fig. 4. Frequency responses from the motor-side input current to the motor side angle.

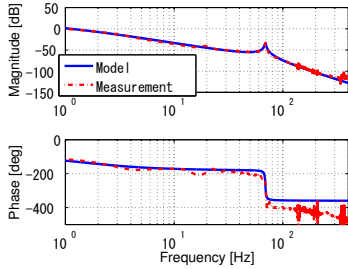


Fig. 5. Frequency responses from the motor-side input current to the load side angle.

Table 1. Parameters of the two-inertia system motor bench.

Motor-side moment of inertia J_M	1.03e-3	kgm ²
Motor-side viscosity friction coefficient D_M	8.00e-3	Nms/rad
Torsional rigidity coefficient K	99.0	Nm/rad
Load-side moment of inertia J_L	0.870e-3	kgm ²
Load-side viscosity friction coefficient D_L	1.71e-3	Nms/rad

possible, a novel control method including the high backdrivable control method using load-side encoder and backlash is proposed. By comparing the geared system with a load-side encoder and without a load-side encoder, the advantages of the system with a load-side encoder for achieving human-machine interactive motion are shown theoretically and experimentally.

This paper is organized as follows. An experimental setup is introduced and modeled in Section 2. In Section 3, the proposed method is explained in detail. In Section 4 and 5, control performance of the proposed method is analyzed in simulations and experiments. Finally, conclusions are given in Section 6.

2. Experimental setup

In this paper, for basic consideration, only one axis movement is considered. Therefore, an experimental setup, which consists of two motors with 20 bits high resolution encoders

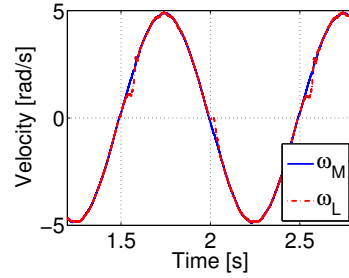


Fig. 6. Experiment for identification of backlash.

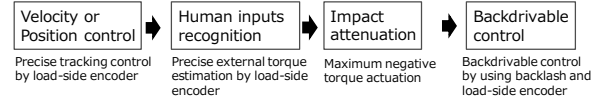


Fig. 7. Overall structure of a proposed human-machine interactive control method.

is used for evaluation. Outlook and a schematic of the setup are shown in Fig. 1 and 2, respectively. To imitate a device with a low frequent resonant mode, a flexible joint can be inserted between two motors. Moreover, by replacing a flexible coupling with a gear coupling, backlash can be added and removed easily.

2.1 Modeling A block diagram of a two-inertia model of the setup is shown in Fig. 3. Let inertia moment, viscosity, torsional rigidity, torque, and angular velocity be denoted as J , D , K , T , and ω , respectively. Subscripts M and L indicate motor side and load side, respectively. Also, motor torque command, motor torque, joint torque, load-side torque, external torque, and torsional angle are indicated as T_M^* , T_M , T_s , T_L , d_L , $\Delta\theta$. Since the current control system is designed such that its control bandwidth is 1 kHz, the dynamics is modeled as the 1st order low-pass filter whose cut off frequency is 1 kHz.

Generally, mechatronic plants include various nonlinearities such as backlashes⁽⁴⁾. In this paper, backlash is modeled as a dead zone and an initial value of $\Delta\theta$ is set as the middle point of the dead zone.

Frequency characteristics of the setup from the motor current to the motor-side angle and the load-side angle are shown in Fig. 4 and 5. These figures show that the setup can be modeled as a two-inertia system whose antiresonance frequency is 57 Hz and resonance frequency is 71 Hz. The parameters identified by the fitting are shown in Tab. 1.

2.2 Backlash identification For backlash identification, motor-side velocity control is implemented. As expressed in (1), backlash can be calculated by integrating the torsional angular velocity between t_1 , when the load separates from the motor side, and t_2 , when the load contacts the motor side again⁽⁹⁾. Let the dead zone width be $\pm\epsilon$.

$$2\epsilon = \left| \int_{t_1}^{t_2} (\omega_M - \omega_L) dt \right| \dots \dots \dots (1)$$

In the experiments, the dead zone width is calculated by not integrating the torsional angular velocity but using the angles at t_1 , t_2 obtained by the encoders on motor and load sides. Figure 6 shows a part of the identification experiments. Averaging the results leads to $\epsilon = 6.0$ mrad.

3. Proposed method for human-machine interactive control

3.1 Overall structure Assuming the application to industrial cooperative robots and welfare robots, the situation that human suddenly pushes the robot during its velocity tracking operation is considered. Cooperative robots are required to behave safe at any time. Therefore, they need to recognize external force inputs and attenuate the impacts between human and machine as soon as possible. In this paper, we assume that robots do not know the timing of the human input beforehand, which means only feedback control can be applied to attenuate the impact. After the contacts between human and robots, robots are controlled to become high backdrivable to follow human's pushing movements. Figure 7 shows an overall structure of a proposed human-machine interactive control method.

3.2 Tracking control Tracking control here indicates any position control or velocity control. Generally speaking, with only a motor-side encoder, it is difficult to achieve good tracking performance at the load side due to low frequent resonant modes and nonlinearities caused by gear reducers. With a load-side encoder, precise tracking control at the load side can be achieved even with unknown nonlinearities in gear reducers.

3.3 Recognition of human inputs: External torque detection Though force/torque sensors can be applied to detect external force/torque by human inputs, the sensors have disadvantages such as high cost, low stiffness, and nonlinearities. Therefore, sensorless estimation is preferred. In this paper, reaction force observer (RFOB) is applied to estimate external torque. When the estimated external torque exceeds the threshold value, which is designed beforehand, robots recognizes that there is a contact with human.

With only a motor-side encoder, as a model used in RFOB, a rigid body model expressed as (3) is used for estimation. Here, subscript n denotes nominal values.

$$P_{alln}(s)^{-1} = J_{alln}s + D_{alln} \dots \dots \dots (2)$$

$$J_{alln} = J_{Mn} + J_{Ln}, \quad D_{alln} = D_{Mn} + D_{Ln}$$

The block diagram of the rigid body model based RFOB is shown in Fig. 8(a). Here, $Q_{RFOB}(s)$ is the 1st order low-pass filter to realize RFOB. When we assume that there is no modeling error for basic consideration, the transfer function from the external torque to the estimated torque is expressed as (3) at the top of the next page. The equation (3) shows that it has resonant characteristics even without any modelling error.

To consider the two-inertia resonant characteristic, RFOB using both motor and load side encoder information is applied⁽¹⁰⁾. The block diagram of the two-inertia model based RFOB is shown in Fig. 8(b). When we assume that there is no modeling error, the transfer function from the external torque to the estimated torque is expressed as (4).

$$\frac{\hat{d}_L}{d_L} = Q_{RFOB}(s) \dots \dots \dots (4)$$

The equation (4) shows an ideal estimation characteristic. Figure 9 shows a characteristic from the external torque to the estimated external torque when the cutoff frequency of

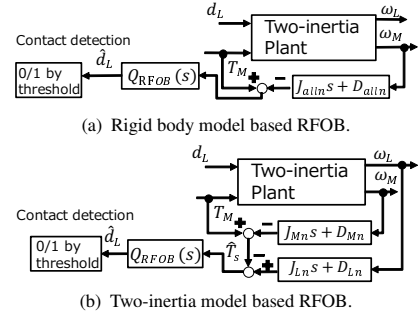


Fig. 8. The block diagrams of the external torque estimation by RFOBs.

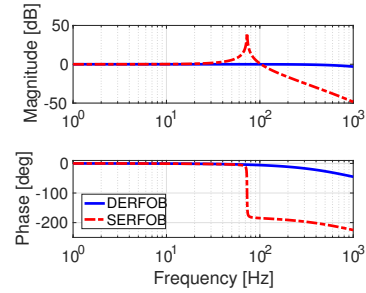


Fig. 9. Frequency characteristics comparison of RFOBs with/without a load-side encoder.

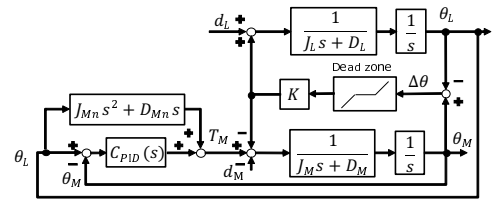


Fig. 10. The block diagram of the high backdrivable control method using a load-side encoder and backlash.

$Q_{RFOB}(s)$ is designed as 1 kHz. The legend DERFOB indicates a double encoders RFOB, which uses both the motor and load side encoders, while SERFOB indicates a single encoder RFOB, which uses only a motor-side encoder. While, the response of DERFOB indicated in blue-and-solid line shows an ideal characteristic, the response of SERFOB indicated in red-and-dashed line has a large peak at the resonance because its estimation model does not consider two-inertia resonant characteristic. The response in high frequency range is important to detect the contact as fast as possible in order to attenuate the impact as much as possible. Moreover, it is not easy to design the proper threshold value with the resonant characteristics in SERFOB. Load-side encoders enable robots to detect the contacts faster by considering resonant characteristics, which enables to robots to attenuate the impact more.

3.4 Impact attenuation As an impact attenuation control method, impedance control is well known. However, it is clear that the maximum braking the actuator can do is the best impact attenuation method we can do in feedback control. Therefore, it is important to detect the contact as fast as possible to actuate the maximum negative torque to attenuate the impact, which means that the load-side encoder has an important role as discussed in the previous subsection.

$$\frac{\hat{d}_L}{d_L} = Q_{RFOB}(s) * \frac{J_{all}Ks + D_{all}K}{J_M J_L s^3 + (J_M D_L + J_L D_M)s^2 + (J_M K + D_M D_L + J_L K)s + (D_M K + D_L K)} \quad (3)$$

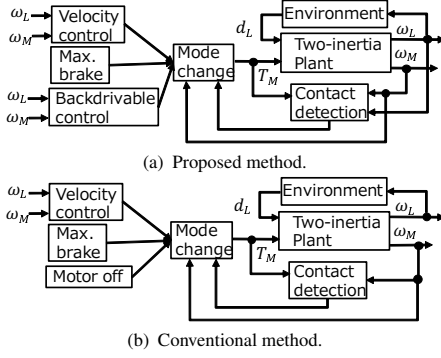


Fig. 11. The block diagrams of the proposed and conventional methods.

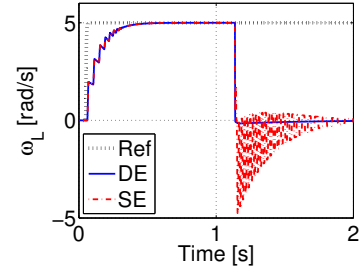
3.5 High backdrivable control using a load-side encoder and backlash

For human-machine interaction, high backdrivability is required to move and follow the human's inputs flexibly. By using load-side encoder information and backlash actively, high backdrivability can be achieved with the method proposed in the literature⁽⁸⁾. When human inputs external force from the load side, the load is hard to move because the friction and the impedance of the gear reducer and the motor are amplified by the gear ratio. Within the backlash width, human feels only the load-side impedance since the load is not connected with the motor. To use this idling characteristic, when external force is input, the proposed high backdrivable control method controls a motor-side position such that the motor side follows the load side within the backlash width.

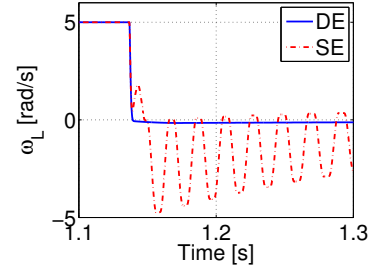
The block diagram of the high backdrivable control method is shown in Fig. 10. Let subscript $C_{PID}(s)$ be denoted as PID controller. The high backdrivable control method is a motor-side position control whose command value is the load-side position obtained by the load-side encoder. In the operating range of the high backdrivable control method, a plant model becomes the only motor-side model because the motor side and the load side are separated by the backlash. Therefore, the FF controller and the PID controller of the high backdrivable control method can be designed only based on the motor-side plant parameters, which makes the method robust against the load-side plant parameters variation. This is a strong advantage in robots since the load-side inertia varies depending on their postures. The advantages of the high backdrivable control method are evaluated with the comparison to the impedance control in the literature⁽⁸⁾.

4. Simulations

4.1 Simulation conditions As stated in the previous section, assuming the application to industrial cooperative robots and welfare robots, the situation that human suddenly pushes the robot during its velocity tracking operation is considered. Since the advantages of the high backdrivable control method using load-side encoder and backlash has been already confirmed in the literature⁽⁸⁾, the simulations and the



(a) Load-side velocity with the contact to the environment.



(b) Zoom of Fig. 12(a).

Fig. 12. Comparison of the load-side velocity responses in the simulations.

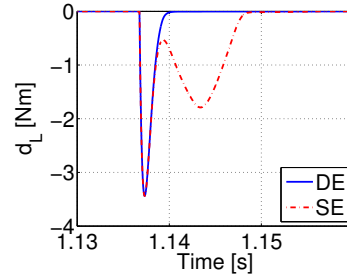


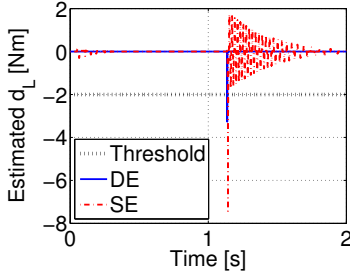
Fig. 13. Load-side external torque in the simulations.

experiments in this paper focus on the other control parts explained in the previous section. Therefore, the backdrivability itself is not evaluated here but the other advantages that can be obtained by using a load-side encoder are mainly evaluated.

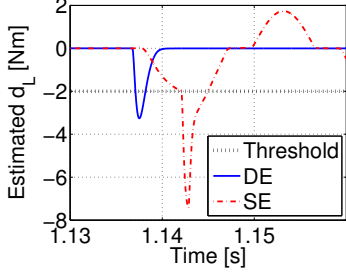
The control structure schematics of the proposed method and the conventional method are shown in Fig. 11

In the proposed method, as a tracking controller, PI-P controller, which consists of the load-side velocity PI controller and the motor-side P controller is implemented. Then, DERFOB is applied to detect the external torque. When the estimated value exceeds the designed threshold value (-2 Nm), the maximum negative torque (-5 Nm) is input to attenuate the impact. After the maximum braking, when the motor-side velocity becomes zero, the high backdrivable control method is turned on.

In the conventional method, we assume that the system does not have a load-side encoder. However, to have the same condition at the impact, the same PI-P controller, which uses



(a) Estimated external torque.



(b) Zoom of Fig. 14(a).

Fig. 14. Estimated external torque in the simulations.

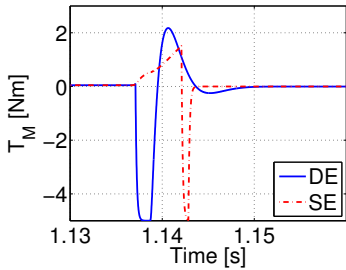


Fig. 15. Motor torque in the simulations.

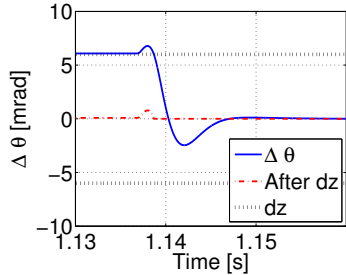


Fig. 16. Torsional angle of the proposed method in the simulations.

a load-side encoder information is implemented. Then, SER-FOB is applied to detect the external torque. When the estimated value exceeds the designed threshold value, the maximum negative torque is input to attenuate the impact. After the maximum braking, when the motor-side velocity becomes zero, the system is turned off for emergency stop (i.e. the control output is zero).

Normally, cooperative robots have soft covers around their surface in order not to injure workers. Therefore, a spring and damper impedance model is used to simulate an impedance between the robots with soft covers and human. The value of the torsional rigidity and the damping coefficient of the impedance model are designed as 1 Nm/rad and 1 Nms/rad,

respectively. The impedance model is placed at the 5 rad distance from the initial position.

There are no modeling errors in simulations. A step velocity reference is filtered with the 1st order low pass filter whose cut off frequency is 50 Hz. The PID controller in the high backdrivable control method is designed such that the poles are placed at 60 Hz. The 2nd order low-pass filter $Q_{FF}(s)$ is applied to make the FF controller proper. The cut off frequency of $Q_{RFOB}(s)$ and $Q_{FF}(s)$ are designed as 1 kHz and 700 Hz, respectively.

4.2 Comparisons in simulations The control performances of the proposed method indicated in blue-and-solid line (legend: DE) and the conventional method indicated in red-and-dashed line (legend: SE) are compared. ω_L responses are shown in Fig. 12. There is a contact between plant's load side and the impedance model around 1.137 s. In the conventional method, ω_L has a large vibration due to the collision between the motor and load sides after the system turns off, while the proposed method has no vibration because the high backdrivable control method moves the motor side to follow the load side.

Figure 13 shows the external torque caused by the contact between the plant and the spring-damper impedance model. The proposed method decreases the impulse, which is calculated by the multiplication of force and time. This means that the proposed method can reduce the thickness of the soft cover of cooperative robots.

Figure 14 shows the estimated external torque. Please note that the true value of the external torque is shown in Fig. 13. By considering the resonant characteristics, the proposed method can detect the contact faster than the conventional method by about 5 ms. Moreover, the conventional method has a large vibration due to the resonance.

Figure 15 shows the motor torque response around the contact to the impedance model. The motor torque in the proposed method quickly goes to the maximum negative torque (-5 Nm) and then, when the motor-side velocity becomes zero, the proposed high backdrivable control method is turned on. To make the motor-side angle follow the load-side angle, the positive torque is input. It is clear that the torsional angle is suppressed within the backlash width (the dead zone is indicated as dz in the legend) as shown in Fig. 16. On the other hand, the motor torque in the conventional method goes up gradually even after the contact because SERFOB still cannot detect the contact. Then, the motor torque quickly goes to the maximum negative torque and then, it is turned off for emergency stop.

5. Experiments

In the experiments, the spring-damper impedance model is implemented by using the load-side motor. The external torque is measured by the torque reference of the load-side motor. The sampling frequency is 2.5 kHz and the controllers are discretized by Tustin conversion. Please note that the threshold value for the contact detection is changed to -3 Nm experimentally.

Figure 17 shows the comparison of ω_L responses. The experimental results are similar to the simulation ones shown in Fig. 12(b). The conventional method has a large vibration while the proposed method shows a good response.

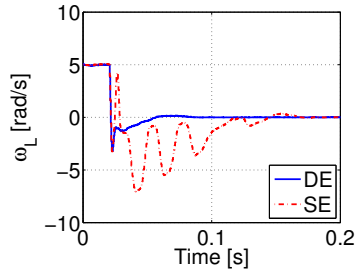


Fig. 17. Load-side velocity in the experiments.

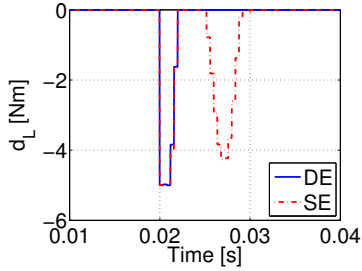
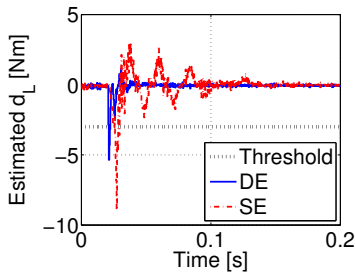
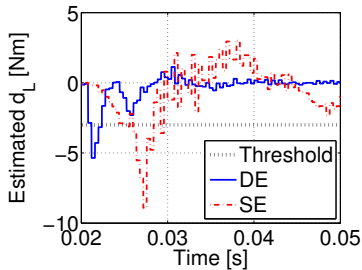


Fig. 18. Load-side external torque in the experiments.



(a) Estimated external torque.



(b) Zoom of Fig. 19(a).

Fig. 19. Estimated external torque in the experiments.

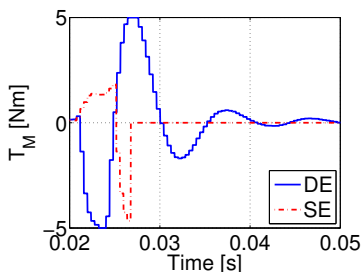


Fig. 20. Motor torque in the experiments.

Figure 18 shows the external torque caused by the contact between the plant and the impedance model implemented in the load-side motor. The proposed method decreases the impulse calculated by the multiplication of force and time.

Figure 19 shows the estimated external torque. The conventional method has a large vibration due to the resonance. The proposed method can detect the contact faster than the conventional method by about 4 ms in the experiment.

Finally, Fig. 20 shows the motor torque response around the contact. The experimental results are similar to the simulation ones shown in Fig. 15. We can confirm that the mode switching algorithm for human-machine interactive motion properly works also in the experiment.

6. Conclusions

Based on the trend of increasing load-side encoders in industry, the human-machine interactive control method using load-side encoder information and backlash is proposed. Although backlash is known to be difficult to deal with, only in terms of backdrivability, backlash has an ideal characteristic. The proposed method uses this characteristic that the load side idles in the backlash width to enhance backdrivability. Moreover, compared to the robots without a load-side encoder, the advantages of applying an encoder to the load side of cooperative robots are shown in the several phases: tracking control, recognition of human inputs, impact attenuation, and high backdrivable control. The proposed method's advantages are verified in simulations and experiments.

7. Acknowledgments

The contributions of DMG MORISEIKI Co., Ltd. are gratefully acknowledged for building the experimental setup. This project was also supported by JSPS KAKENHI Grant Number 16J02698.

References

- (1) G. B. Avanzini, N. M. Ceriani, A. M. Zanchettin, P. Rocco, and L. Bascetta: "Safety Control of Industrial Robots Based on a Distributed Distance Sensor", *IEEE Trans. Control Syst. Technol.*, Vol. 22, No. 6, pp. 2127–2140, (2014).
- (2) K. Kong, J. Bae, and M. Tomizuka: "A Compact Rotary Series Elastic Actuator for Human Assistive Systems", *IEEE/ASME Trans. Mechatronics*, Vol. 17, No. 2, (2012).
- (3) K. Yuki, T. Murakami, and K. Ohnishi: "Vibration Control of 2 Mass Resonant System by Resonance Ratio Control", *Proc. the IEEE Annu. Conf. the IEEE Ind. Electron. Soc. (IECON)*, pp. 2009–2014, (1993).
- (4) M. Iwasaki, M. Kainuma, M. Yamamoto, and Y. Okitsu: "Compensation by Exact Linearization Method for Nonlinear Components in Positioning Device with Harmonic Drive Gearing", *J. JSPE*, Vol. 78, No. 7, pp. 624–630, (2012).
- (5) M. Nordin and P. Gutman: "Controlling mechanical systems with backlash – a survey", *Automatica*, Vol. 38, pp. 1633–1649, (2002).
- (6) D. K. Prasanga, E. Sariyildiz, and K. Ohnishi: "Compensation of Backlash for Geared Drive Systems and Thrust Wires Used in Teleoperation", *IEEJ J. Ind. Appl.*, Vol. 4, No. 5, pp. 514–525, (2015).
- (7) S. Yamada, K. Inukai, H. Fujimoto, K. Omata, Y. Takeda, and S. Makinouchi: "Joint torque control for two-inertia system with encoders on drive and load sides", *Proc. the 13th IEEE Int. Conf. on Ind. Informat. (INDIN)*, pp. 396–401, (2015).
- (8) Shota Yamada and Hiroshi Fujimoto, "Proposal of High Backdrivable Control Using Load-Side Encoder and Backlash", *Proc. the 42nd Annu. Conf. the IEEE Ind. Electron. Soc. (IECON)*, pp. 6429–6434, (2016).
- (9) S. Villwock and M. Pacas: "Time-Domain Identification Method for Detecting Mechanical Backlash in Electrical Drives", *IEEE Trans. Ind. Electron.*, Vol. 56, No. 2, (2012).
- (10) C. Mitsantisuk, M. Nandapaya, K. Ohishi, and S. Katsura: "Design for Sensorless Force Control of Flexible Robot by Using Resonance Ration Control Based on Coefficient Diagram Method", *Automatica*, vol. 54, no. 1, pp. 62–73, (2013).